Phyto-Assisted Synthesis of Bio-Functionalized Ag/Ag_2O Nanoparticles, Characterization, Optical and Their Potential Anti-Oxidants Activities

Mohamed Bilal Goudjil[1,4*], Fatma Zohra amar Ayachi[1,4] , Souad Zighmi[2,4] , Zineb Mahcene[3]

[1]Applied Sciences Faculty, Process Engineering Laboratory, Ouargla University, Ouargla 30000, Algeria
[2]Applied Sciences Faculty, Engineering Laboratory of Water and Environment in Middle Saharian Laboratory, Ouargla University, Ouargla 30000,Algeria
[3]Sciences of the nature and life Faculty, Protection of Ecosystems in Arid and Semi-Arid Zones Laboratory, Ouargla University, Ouargla 30000, Algeria

[4]Ouargla University, Applied Sciences Faculty, Process Engineering Department, Ouargla 30000, Algeria

***Correspondence : E-mail*:** goudjil.bilal@univ-ouargla.dz,

ORCID iD:https://orcid.org/0000-0001-8125-4405

Received :13-06-2023 **Accepted :**03-01-2024 **Published :** 31-01-2024

Abstract :

In this study, green synthesis of silver/ silver oxide nanoparticles (Ag/Ag_2O NPs) was achieved by bio-reduction of silver nitrate using *Mentha Piperita* plant leaves extract.The effect of different silver nitrate concentrations on the formation ofsilver nanoparticleswas studied. The obtained nanoparticles were characterized using UV-Vis, FT-IR, XRD, and SEM techniques. The antioxidant activity of samples was evaluated using three methods: the DPPH test (2,2-diphenyl-1-1-picrirylhydrazil), the FRAP (Ferric reducing antioxidant power) and TAC (Total Antioxidant Capacity) test. UV-Vis spectra showed maximum absorption in the range of 253–300 nm related to the silver. FTIR spectra exhibit a weak peak at 565 cm^{-1} attributed to silver NPs vibration, confirming the nanoparticles formation. The X-Ray Diffraction (XRD) analysis confirmed the crystalline nature of (Ag/Ag_2O NPs) with an average size ranged in 31–42 nm. SEM showed that the green synthesizing silver nanoparticles having in general as cubical shape. Among the examined extracts, (Ag/Ag_2O NPs) with 1g concentration showed the highest antioxidant activity with value of 2.749, 21.60 and 18.69 mg/ml for DPPH, FRAP and TAC tests respectively. Consequently, the use of peppermint leaves extract offers a convenient, rapid, cost-effective, and environmentally friendly alternative to other methods. The research findings from the various assays measuring antioxidant capacity clearly demonstrate that the silver nanoparticles produced by M. Piperita possess potent natural antioxidant properties that are beneficial for preserving health.

Keywords: Biomaterials;Green synthesis; Nanoparticles;*Mentha Piperita*; $AgNO_3$; XRD

Tob Regul Sci.™ 2024;10(1): 330 - 350

DOI: doi.org/10.18001/TRS.10.1.23

1. Introduction

Medicinal plants are both a finished product for consumption and a raw material for obtaining bioactive substances that are at the origin of several modern medicines due to their richness in secondary metabolites, especially phenolic compounds with beneficial biological properties.Currently, the emergence of nanotechnology, which refers to the production at the nanometric scale (1 to 100 nm) of materials or products of controlled sizes and structures, is the consequence of the appearance of new physicochemical properties more advantageous and unique physicochemical properties that differ greatly from other materials due to the small size of the charges. These performances have contributed to radical changes in various fields of technology and science [1].

Plant products find imperative use in the synthesis of nanoparticles (NPs). Silver(Ag) is the metal of choice among noble metals for potential applications in biological systems, organic matter and medicine [2-6].

Among the plants with important pharmacological potentialities, *Mentha piperita* which is widely spread and used in Algeria. Their biological activities are closely linked to their richness in active substances, which they contain such as phenolic compounds.

In order to better understand the interest of bioactive substances of *Mentha piperita*, it seemed useful to us to undertake this present work which deals with the synthesis of silver nanoparticles using the extract of this plant.

In this study, green synthesis method was used which have emerged as a quick and simple approach to synthesis, inexpensive, environmentally friendly and cost-effective. we prepared silver nanostructures using different weight of silver nitrate directly in leaf extract solution and investigated their structural, morphological, optical, and antioxidant properties.

2. Materials and methods

2.1. Preparation of the leaf extract:

The plant material that is used during the realization of this work consists of *Mentha Piperita*leaves species collected in March 2023 in the region of Tiaret (Western Algeria) coordinates (N 35.362222 °E 1.285555 °). Fresh leaves were subjected to a shade drying process at room temperature for a duration of 5 days, followed by crushing to obtain a finely powdered

form. The extract was prepared by putting 40g of powder's leaves with 400ml of distilled water in a 500ml glass beaker. In addition, magnetic stirring at 350 rpm and heating at a temperature of 90°C is carried out for 1 hour. The extract was filtered using a filter paper (Whatman No: 2) and stored at 4°C for further use.

2.2. Synthesis of Silver nanoparticles by *Mentha Piperita*extract

Silver nanoparticles were synthesized by a modified protocol from previous researches [4, 7, 8]. Briefly, by adding with four different weight (0.1, 0.6, 0.9, and 1g) of the silver nitrate ($AgNo_3$) to the 100 ml leaf extract in a 250 ml flask. AgNPs were immediately obtained with the reduction process. For one hour, the mixture was continuously stirred at 75 C. The transition from bright yellow to dark brown is an indication that silver nanoparticles are forming. The reasonable mechanism of silver nanoparticles formation may be due to the reduction of silver ions that takes place together with the phenolic compounds in theM. Piperita leaf extract.

2.3. Characterization of silver nanoparticles

Several techniques have been used for the characterization of silver nanoparticles such as: UV-Vis, FT-IR, XRD and SEM and EDX.

2.3.1. UV–Visible Spectroscopy

The device is the HACH DR6000 UV-Vis spectroscopy, which operates in the wavelength range of 190 to 1100 nm. The samples were analyzed in a quartz cell. Thespectrophotometer enclosure was thermostated at 25°C and distilled water was used as the reference solvent.

2.3.2. FTIR Spectroscopy

This technique was used to identify the functional groups present in a sample as well as the bonds developed after the formation of silver nanoparticles. The powder of silver nanoparticles prepared from leaf extract was deposited in the ATR (Attenuated Total Reflectance) spectroscopy.

2.3.3. X-ray Diffraction (XRD)

The structure and grain size of AgNPs were examined by XRD techniques using Xray diffractometer (BTX-716) with a Cu-Ka (k = 1.5406 A˚) in 2θ range of 5-70,whereas X-ray was generated with 30 kilovolts andat 20mA.

2.3.4. Scanning Electron Microscopy (SEM)

The surface morphology of all studied samples was observed by EVO-15 SEM (EVO 15, ZEISS, Germany) using an acceleration voltage of 15 kV supported with an energy dispersive X-ray Spectroscopy (EDX).

2.4. Antioxidant Activity

2.4.1. Free radical scavenging effect

The DPPH test (diphenyl picrylhydrazyl) is a widely used method in the analysis of the antioxidant activity. This method is utilized to evaluate the scavenger effect of the leaf extarct of plant and Ag/Ag_2O Nps against DPPH radical was according to literature [9, 10],with some modifications (samples diluted in absolute ethanol). 1 ml of sample at different concentrations diluted in ethanol were added to 1 ml of the DPPH solution prepared at 0.4 mM in ethanol. After 30 min of incubation in the dark, the absorbance reading at 517 nm; The mixture of 1 ml of the DPPH solution and 1 ml of ethanol is taken as control product.The reduced level of these molecules by DPPH is expressed in percentage according to the following formula:

$$I\,\% = \left({A_0 - A_e}/{A_0}\right) \times 100$$

In which A_0 is the absorbance of the control reaction and Ae is the absorbance of the Sample.

As for the inhibitory concentrations (IC_{50}), they are calculated from the curves of linear regression. Tests were carried out in triplicate.

2.4.2. Ferric reducing power

The iron reducing activity of samples was determined according to the method described by Oyaizu [11]. A volume of 2.5 ml of phosphate buffer (0.2M, pH 6.6) was added to a 1 ml of various concentrations of Leaf extract and Ag/Ag2O NPs. 2.5 ml of potassium ferricyanide are added after it (1%). The mixture was stirred, then incubated for 20 minutes at 50°C. Then, 2.5 mL of 10% trichloroacetic acid was added to the mixture, which underwent a 10 minute centrifugation at 3000 rpm. After that, 0.5 mL ferric chloride (0.1%) and 2.5 mL of distilled water were added to this mixture, and it was violently stirred. At 700 nm, the absorbance was finally measured. Ethanol was used to dilute the samples. Similar to the extracted sample, a blank sample is made by substituting ethanol, which is used to calibrate the instrument (UV-VIS spectrophotometer). The EC_{50} value, which was calculated by interpolating using linear regression analysis, is the effective concentration at which the absorbance was 0.5 for reducing power [12]. Increased absorbance of the reaction mixture indicated an increased reducing power [13].The tests were conducted in triplicate.

2.4.3. Total antioxidant activity (TAC)

The total antioxidant capacity (TAC) of the extracts is evaluated by the phosphomolybdenum method[14]. It is based on the reduction of molybdatesMoO_4^{2-} to Molybdenum$Mo(V)MoO^{2+}$ions in the presence of extracts, giving a green color detectable by UV-visible light at a wavelength of 695nm.

A volume of 0.2ml of each ethanoic extract is mixed with 2ml of reagent solution (0.6M sulfuric acid, 28mM sodium phosphate and 4 mM ammonium molybdate). The tubes are screwed on and incubated at 95° C. for 90 min. After cooling, the absorbance of the solutions is measured at 695 nm in comparison to a blank that has been incubated under the same circumstances as the sample and includes 2 ml of the reagent solution and 0.2 ml of ethanol. The effective concentration that lowers molybdenum to an absorbance of 0.5 is known as the EC_{50} value. It is obtained using interpolation from the linear regression analysis.

Results and discussion

Mentha Piperita-mediated synthesis of Ag/Ag_2O NPs is more advantageous than chemical and physical synthesis because it is a clean, non-toxic, cost-effective, and environmentally friendly approach. In addition, Mentha Piperita is widely available in nature, making it a preferable plant material for industrial scaling up [15-18].

Phytochemical analysis of *Mentha piperita* leaf extract revealed that they contain polyphenols, flavonoids, tannins, and saponins [19-21].

The color shift of the solution from yellow to dark brown in less than an hour is the most significant visual observation during the reaction. The production of Ag/Ag_2O NPs is clearly indicated by the brown color. Based on this evidence, a possible mechanism for Ag^{2+} reduction and Ag/Ag_2O NPs formation were proposed using *Mentha piperita* leaf extract.

During synthesis, plant leaf extracts that rich in polyphenol content are employed as bioreducing agents. The reduction process consists of transforming Ag^{2+} ions into Ag^0. The Ag^0 represented by the AgNPs is transformed into Ag/Ag_2O NPs after annealing in the incinerator at 500°C for 2h [22].

2.5. UV–visible Spectroscopy

UV-Vis spectra of Ag/Ag_2O nanoparticles synthesized using a peppermint extract are shown in Fig. 1. As can be seen in this figure, a maximum absorption peak is presented from the interval of 253 to 300 nm which gives a clue that silver/silver oxide nanoparticles may be formed [8, 23].Moreover, the strong absorption peak can be caused by the collective oscillation of the electrons in the free conduction band which is excited by the incident electromagnetic radiation.

Furthermore, as seen, the samples' absorption intensity increased as the silver concentration increased. This shows that the amount of nanoparticles produced as a result of silver ion reduction has increased[24-26].

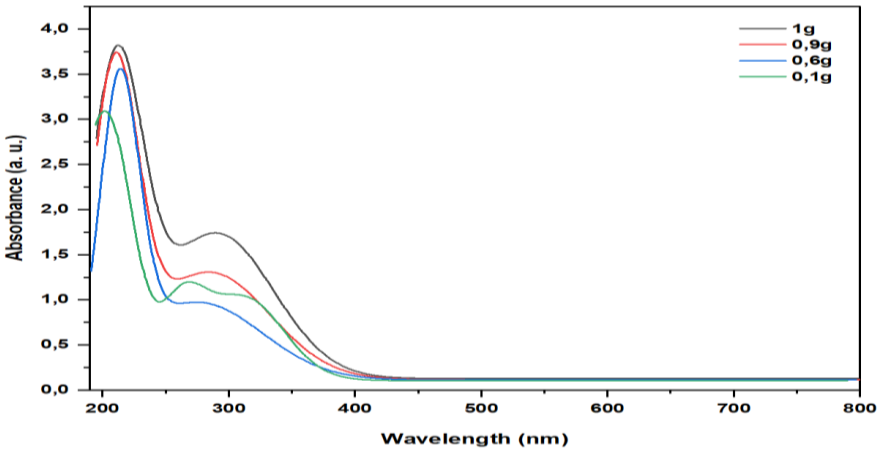

Fig. 1. UV–Vis absorption spectrum of Silver nanoparticles synthesized.

2.5.1. Estimation of the optical band gap:

Generally, the estimated optical energy band of a silver nitrate nanoparticle semiconductor (Eg) can be determined by extrapolation from the absorption band using the Tauc relation (Equation (1))[27] :

$$(\alpha h\nu) = A(h\nu - E_g)^n \qquad (1)$$

Where α is the absorption coefficient, A is constant, $h\nu$ is the incident photon energy, and n is a constant depending on the nature of the electronic transition (n = 1/2 for indirect transition, n = 2 for direct transitionas shown in Figure 2) , Eg is the optical band gap energyin electron-volts (eV), and the exponent n = 1/2 for the direct allowed transition (Figure (2))We obtained the energy gap from the intersection of the edge of the linear absorption part with the energy axis[28, 29].

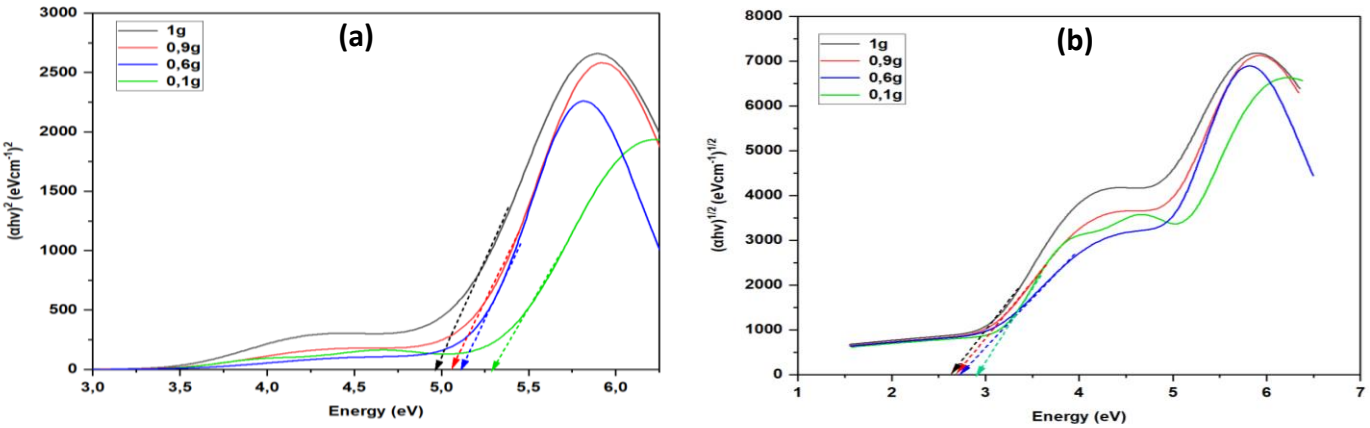

Fig. 2. Determination of optical energy gap for (a) direct and (b) indirect bandgapstransition using Tauc's method.

Generally, several factors can affect the band gaps of prepared Ag/Ag_2ONPs, i.e., crystallinity, crystallite size, particle size, particle shape and composition [30]. Low band gap energies allow Ag/Ag_2ONPs to absorb the vast majority of the solar spectrum, and direct band gaps give Ag/Ag_2ONPs a large absorption coefficient.

As shown in Table 1, the AgNo3 concentration increases from 0.1g to 1g reflect that both direct bandgap decreases from 5.29 to 4.98 eV, and the indirect bandgap decreases from 2.95 to 2.65 eV. The results are consistent with theliterature review that the bandgap decrease with a increases in concentration [31-33].

2.5.2. Estimation of the Urbach energy:

The Urbach energy is also known as the Urbach tail and can be detected by the UV-vis spectra. The highest value of Urbach energy shows lower crystallinity and disorder in Ag/Ag_2O NPs. The Urbach energy E_u is derived by taking the mutual values of the slopes of the linear part of ln(a) as a function of photon energy (Fig. 3)[34]

$$\ln a = \frac{h\nu}{Eu} + constant\ (\ln a_0) \qquad (2)$$

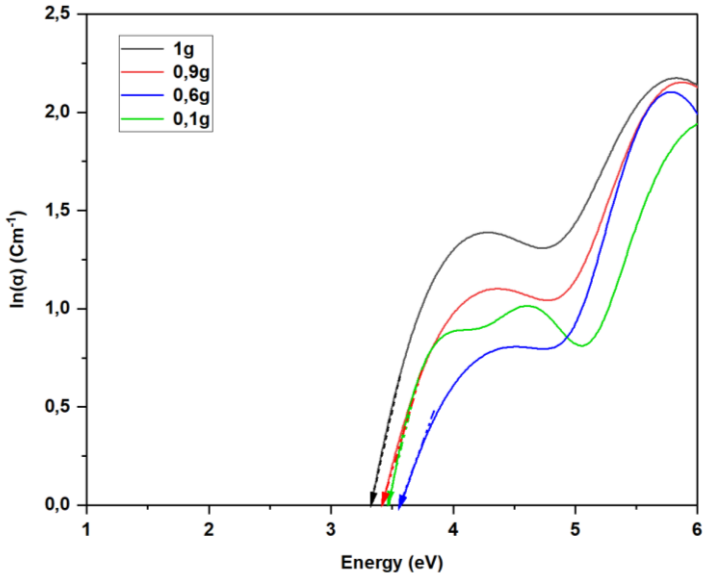

Fig. 3. Urbach energy estimate of the silver nitrate nanoparticles synthesized by the extract of *Mentha piperita* leaf

The estimated Urbach energy values for the samples are presented in Table 1.The results indicated thatthe Urbach energy of the Ag/Ag_2O NPs slightly decreases from 0.67 to 0.36 eV with the increase in the particle sizeand the increase in silver nitrate concentrations. These results were explained for Urbach energy due to the effect ofstructural and thermal perturbation.

Table 1 The values of direct band gap, indirect band gap and Urbachenergy of thebiosynthesizedAg/Ag_2O.

Samples	Direct Optical band gap (eV)	Indirect Optical band gap (eV)	Urbachenergy (eV)
0.1g	5.29± 0.21	2.95± 0.47	0.66± 0.58
0.6g	5.12± 0.37	2.79± 0.73	0.50± 0.42
0.9g	5.05± 0.11	2.70± 0.23	0.43± 0.38
1g	4.98± 0.17	2.65± 0.19	0.36± 0.41

2.6. Fourier Transform Infrared spectroscopy(FTIR)

The FT-IR analysis was used for both *Mentha Piperita* leaf extract and synthesized silver nanoparticles solution before annealing at 500°C to identify the possible biomolecules responsible for Ag/Ag_2O Nps synthesis.

The study was carried out by FTIR spectrophotometer (Cary670) in the frequency range 4000-400 cm^{-1} for *Mentha Piperita*leaf extract with different spectra of nanoparticles prepared with different ration (Figure 4). The result of FTIR spectrum exhibited several absorption bands that correspond to the functional groups of the biomoleculesexisting in the plant extract. Main absorption peaks were observedat 3300, 2900, 1740, 1606, 1417, 1026 and 565 cm^{-1}. The broadband, at 3300 cm^{-1}, is due to the OH group stretching vibration. Significant peaks were observed at wavenumbers of 2960 and 2871 cm^{-1}, which can be attributed to the stretching vibrations of the C-H bonds in the methyl group. The absorption peaks located at approximately 1740 and 1417 cm^{-1} are indicative of the stretching vibrations of the C=C, C-C, and C-O bonds in the aromatic cycles.Thepeak located at 1026 are assigned to the stretching band of C-O. Weak bands at 565 cm^{-1} silver nanoparticles solution before annealing indicate to the Ag-O stretching band of Ag/Ag_2O Nps[35-37].

The comparison between the IR spectra of *Mentha Piperita* extract before and after the addition of silver nitrate shows that:

A decrease in the intensity of the broad band from 3300 cm^{-1} to 2900 cm^{-1} which represent the free OH groups in the molecule, , this group reacts to reduce Ag+ in reaction media which leads to the formation silver nanoparticles according to several authors [38-40]

An appearance of a 1740 cm^{-1} peak is observed corresponding to the(C=O) grouping.

Also, an appearance peak is observed at 565 cm^{-1} attributed to the Ag/Ag2O Nps binding of silver nitrate.

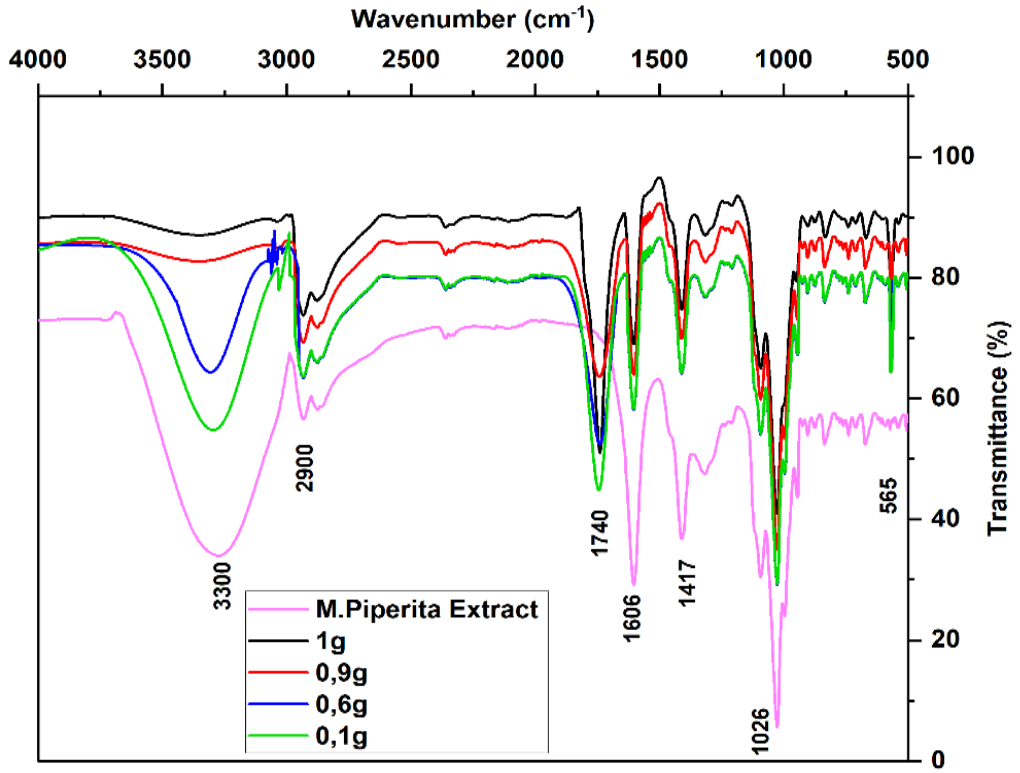

Fig. 4. FT-IR spectra of M. Piperita leaf extract and as synthesized silver nanoparticles solution before annealing with different silver nitrate concentration.

2.7. Crystal structure and crystallite size

XRD patterns of synthesized AgNPs Prepared using the *Mentha Piperita* leaf extract and various concentrations of silver nitrateafter annealing at 500°C are shown in Figure 5.

The diffraction pattern confirms the presence of two crystalline phases, Silver (Ag) and Silver oxide (Ag_2O). The peaks at 2θ values of 38.3°, 44.45°, and 63.95° correspond to the crystalline planes of (111), (200), and (220), respectively, which validate the formation of the face-centered cubic structure.[41, 42] ((ICSD) Card No. 98-005-3759).

The other seven characteristic peaks at 2θ values of 26.09°,32.09°, 37.23°, 46.03°, 53.67°, 63.92° and 67.13° are attributed to the crystal planes of (110), (111), (200), (211), (220), (311) and (222) which correspond to the face-centered cubic structure of silver(I) oxide[43] ((ICSD) Card No. 98-017-4092).

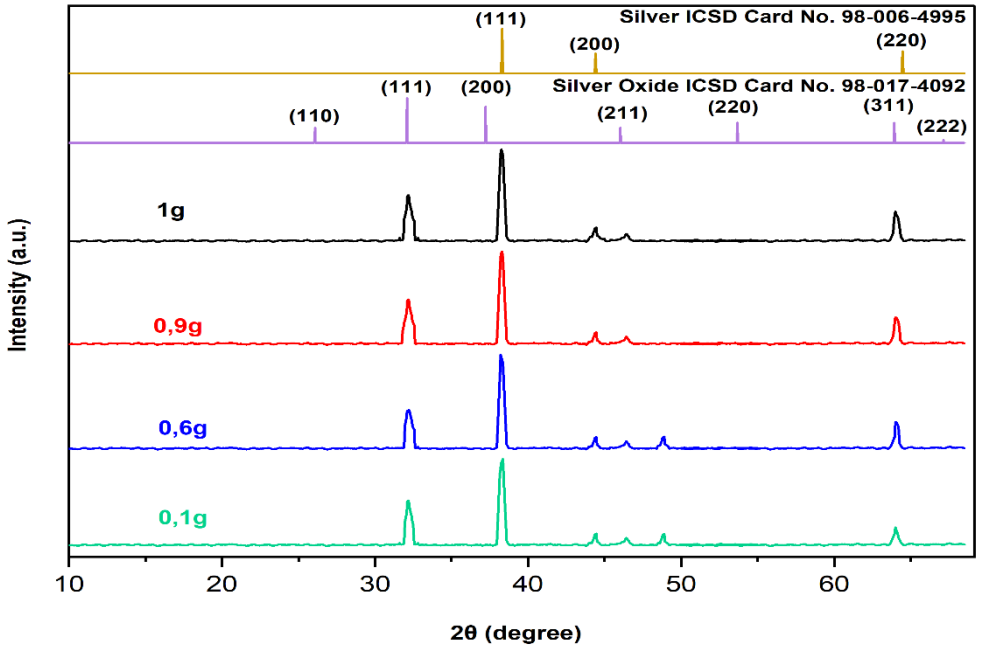

Fig. 5. XRD patterns of Silver/Silver Oxide nanoparticles synthesized

Using the Scherrer formula Eq (3), the average crystallite size of the synthesized nanoparticles was determined by choosing the peaks at 2θ values:

$$D = \frac{K\lambda}{\beta \cos\theta} \qquad (3)$$

Where D is the crystalline size (nm), β is the full width at half maximum of the diffraction peak (FWHM) of the most intense diffraction peak, λ the X-ray wavelength (1.5406 Å) and θ is the Bragg angle of diffraction [44].

Table 2 displays the influence of different concentration on Ag/Ag_2O crystallite size.The findings demonstrated that the concentration ratio has an impact on crystallite size. Noteworthy that the Ag/Ag_2O NPs crystallite size was unaffected by the concentration ratio's increase from 0.9 to 1g. On the other hand, the crystallite size of Ag/Ag_2O considerably fell from 42.52 nm to 34.78 nm when the concentration ratio increased from 0.6 to 0.9g.

Numerous earlier research [45-47] also revealed that reducing the crystallite size by increasing the ratio of surfactant (plant extract) was possible.

2.8. Scanning Electron Microscopy (SEM)

The formation of Ag/Ag_2O NPs and their morphological dimensions were studied using the SEM. Fig. 6 (a–d) exhibits SEM images of the synthesized silver (Ag/Ag_2O NPs). It is observed that most of them are cubic in nature and irregular shaped. Further analysis of silver nanoparticles, by EDAX, as shown in (Fig.6 (4e)) its associated data, confirms the presence of

silver and oxygen, with the weight percentage of about 68.84% Ag and 3.53% O.Results means that most of the particles formed are specific toAgNPs.

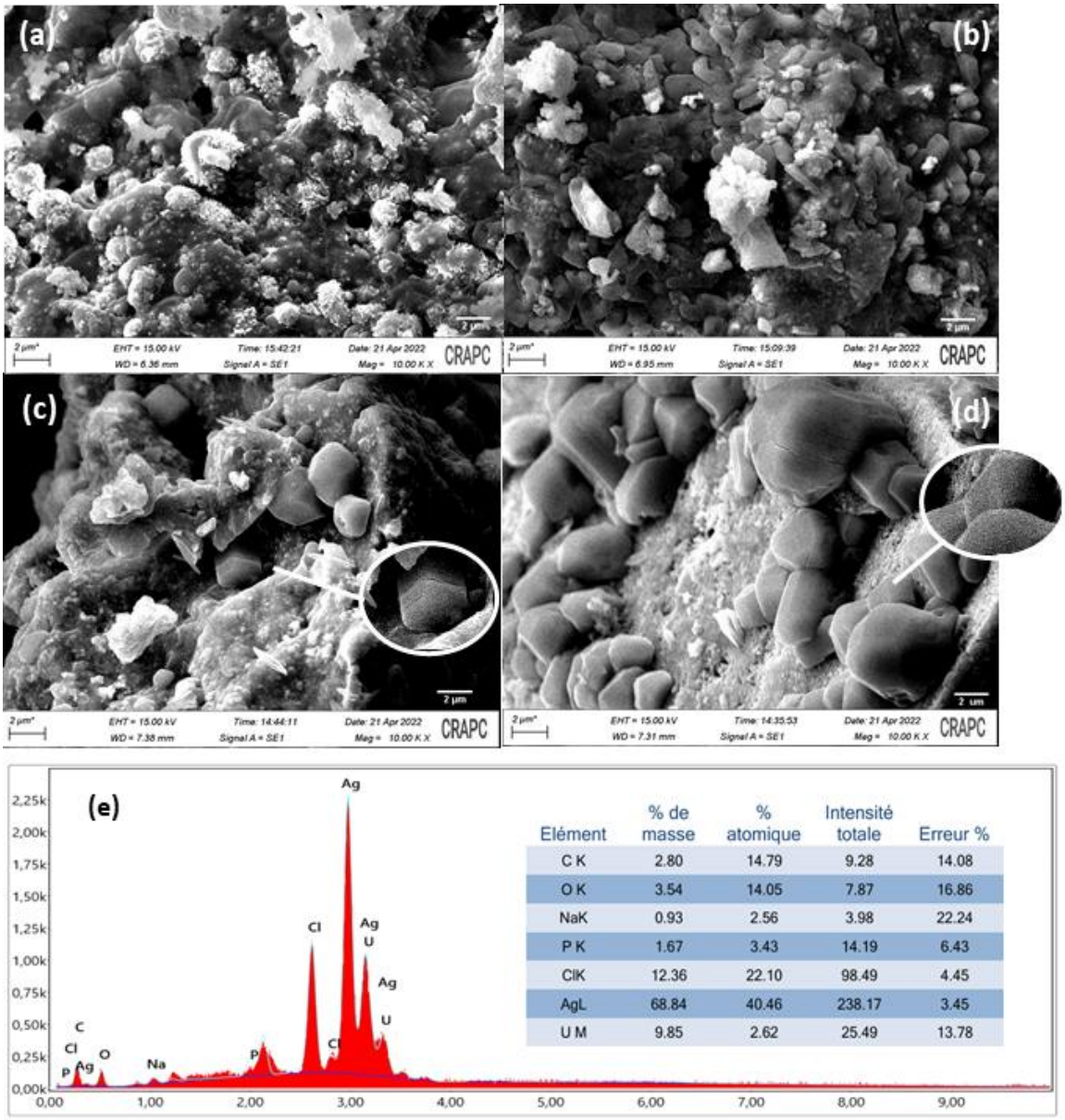

Elément	% de masse	% atomique	Intensité totale	Erreur %
C K	2.80	14.79	9.28	14.08
O K	3.54	14.05	7.87	16.86
NaK	0.93	2.56	3.98	22.24
P K	1.67	3.43	14.19	6.43
ClK	12.36	22.10	98.49	4.45
AgL	68.84	40.46	238.17	3.45
U M	9.85	2.62	25.49	13.78

Fig. 6. SEM images of green synthesized Ag /Ag_2O NPs nanoparticles: a) 0.1 g, b) 0.6 g, c) 0.9 g, d) 1 g and e) EDAX of silver nanoparticles.

2.9. Evaluation of the antioxidant activities

Several techniques were used to evaluate the antioxidant activity. These techniques depend completely on the reduction capacity or the ability to trap free radicals as an indicator of their antioxidant potential [48-51]. Three techniques were used to determine the antioxidant activity of the samples (leaf extract and Ag/Ag_2O NPs) in vitro: the scavenger effect against DPPH

radical, the reduction of iron and the total antioxidant capacity. Results of the antioxidant activities are summarized in figure 6 and table 2

Table 2. Size and The antioxidant activities of Ag/Ag_2O NPs synthesized at different silver nitrate concentration.

Samples	Ag/Ag_2O NPs size (nm)	antioxidant activities (mg/ml)		
		DPPH IC_{50}	FRAP EC_{50}	TAC EC_{50}
Leaf extract	-	7.40± 1.21	49.94± 0.93	128.68 ± 0.44
0.1g	38.49 ± 0.56	7.09± 0.77	37.69± 0.81	62.43 ± 1.42
0.6g	42.52 ± 0.91	6.72± 0.12	32.91± 0.61	29.65 ± 0.66
0.9g	34.78 ± 0.44	4.86± 1.11	25.90± 0.38	19.83 ± 1.15
1g	31.96 ± 0.17	2.74± 0.27	21.60± 0.63	18.69 ± 0.21

3.5.1. Scavenger effect of the radical DPPH

DPPH (2,2-diphenyl-1-picrylhydrazil), one of the first free radicals employed to examine the relation between structure and antioxidant activity, was used to evaluate the antiradical activity. [52].

It is a stable radical solution that is purple and has a typical maximum absorption at 517 nm. The standard procedure is based on the disappearance of the maximum when DPPH is decreased by a chemical with anti-radical abilities, causing the discolouration yellow.

The figure (7 -(a)) below show the effectiveness of the Ag/Ag_2O nanoparticles at different silver nitrate concentration and leaf extract solution to trap the DPPH radical, this efficiency has resulted in the inhibition rate according to the different concentrations.

The samples' IC_{50} values, also known as the 50% inhibitory concentrations, are calculated and listed in Table 2. It is described as the sample concentration necessary to produce a 50% reduction in the initial DPPH solution's absorbance. The scavenger effect's low values, which are negatively correlated with the IC_{50}, indicate a considerable anti-radical impact [53-55].

The results show that the antiradical power has increased as the concentration of silver nitrate has increased. The Ag/Ag_2O Nps, which was made using 1 g of silver nitrate, appears to be the most powerful antioxidantwith 2.75 mg/ml concnetration, as compared to other samples, which had IC_{50} values of 4.86, 6.72, 7.09, and 7.4 mg/ml, respectively (figure 7 (d)).

3.5.2. Ferric reducing power

Previous research has demonstrated that a compound's reducing capacity might be a useful predictor of its prospective antioxidant action. Its fundamental idea is based on a compound's capacity to give an electron.[56-58].The $[K_3Fe(CN)_6]$ complex contains a ferric ion (Fe^{3+}), which when reduced to ferrous (Fe^{2+}) results in the transition of the yellow ferricyanide of potassium into a blue color in a reaction medium at 700 nm, the intensity of which is dependent on the reducing power of the samples.

The results of the Ag/Ag_2O Nps reductive activity at different concentration and leaf extract solution are presented in the curves below (figure 7 -(b)).

As with the antiradical activity, the concentration of the Ag/Ag_2O Nps samples has a highly significant effect on the reducing power. From (figure 7 -(b))., the reducing power is proportional to the antioxidant concentration. Similar observations have been reported by many authors [55, 59-61].

The (figure 7 -(d)) indicates that the Ag/Ag_2O Nps that used 1 g of silver nitrate in preparation has a more effective antioxidant activity than that of other samples and leaf extract solution where the EC_{50} values are 21.6mg/ml. Whereas the leaf extract, 0.9, 0.6 and 0.1 g/AgNo3, gave a value of 49.94, 37.69 and 32.91mg/ml respectively.

3.5.3 Total antioxidant capacity (TAC)

The in vitro antioxidant effect of our Ag/Ag_2ONpsand leaf extract samples was evaluated by total antioxidant capacity (TAC) method ((figure 7 -(c)).The EC_{50} value represents the concentration at which molybdenum is reduced to an absorbance of 0.5. It is determined through interpolation using linear regression analysis. This value is inversely related to the overall antioxidant capacity, with lower values indicating a stronger anti-radical effect.Table 2 illustrate the results of the total antioxidant capacity of different samples at different Silver nitrate concentration. These results show that all samples show significant antioxidant capacity. The 1g sample has the best total antioxidant capacity of the order of 18,977 ± 7,21 mg/mlNPs compared with the other samples and leaf extract sample.
These results can be explained by the fact that the grain size of Ag/Ag_2ONPs and silver nitrate concentration influence the antioxidant power.

By conducting a comparative analysis of the outcomes from the TAC, FRAP, and DPPH assays, it can be deduced that the Ag/Ag_2O nanoparticles synthesized from 1 g $AgNO_3$ exhibit robust antioxidant activity. This finding substantiates the notion that the size of the particles has a notable impact on their antioxidant potential.In similar studies [62-64], researchers evaluated the

antioxidant activity of AgNPs, and by comparing the results obtained, we can say that we got wonderful results.According to the findings of the numerous assays measuring antioxidant capacity, the silver nanoparticles produced by the M. Piperita are potent natural antioxidants beneficial for the health preservation due to their antioxidant capabilities.

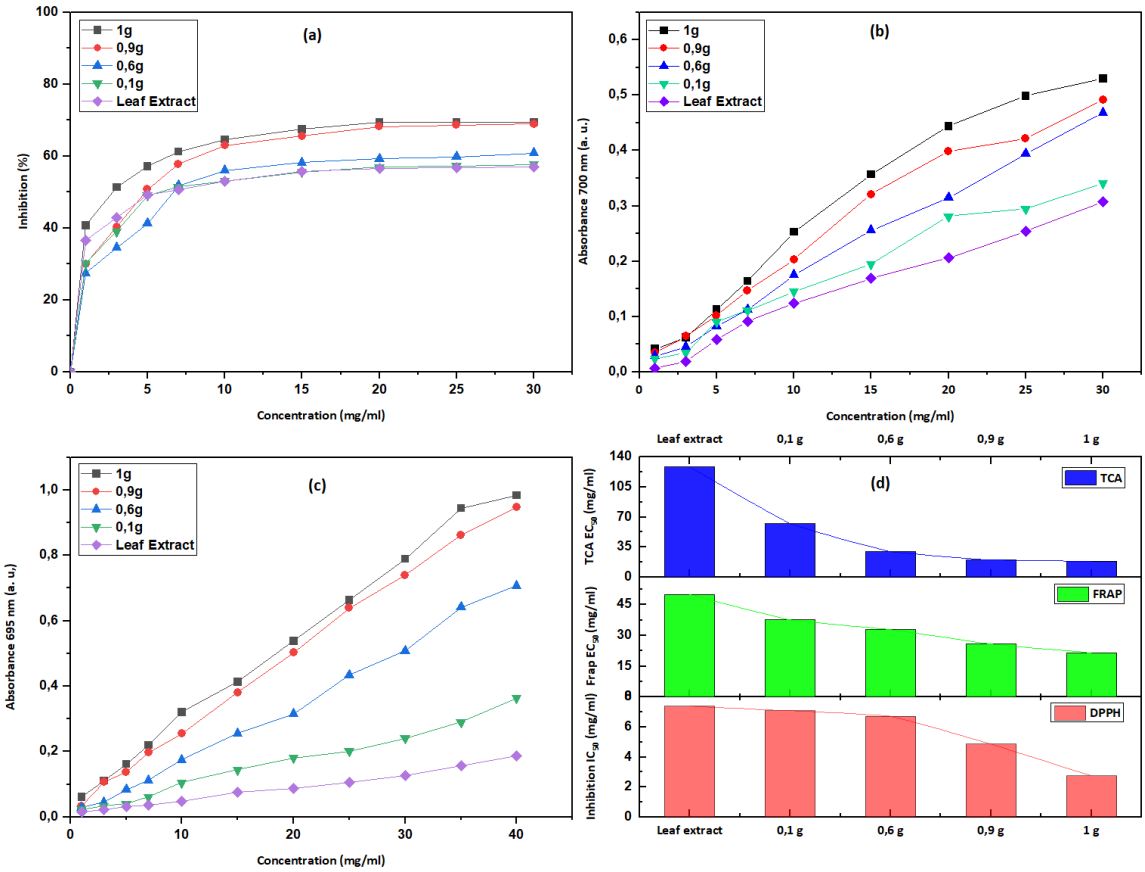

Fig.7.The antioxidant activities of the Ag/Ag_2O nanoparticlesprepared using *Mentha Piperita* leaf extract with different concentrations of AgNO3: a antiradical activity (DPPH) ; b Ferric reducing power(FRAP); c Total antioxidant capacity (TAC); d IC_{50} and EC_{50} of all antioxidants tests.

3. Conclusion

A simple, one-step green approach was devoted for the synthesis of AgNPs.The prepared Ag/Ag_2O NPs product has a cubical structure with an average diameter is 31.96-42.52 nm and exhibited biologicals activities, which could effectively reduce the oxidatationphenomena and might have potential applications in a antioxidation. Results showed the variation of the weight Ag precursor allows us to strictly control the size and shape of the silver nanoparticles, which could be a potential source for the production of highly efficient antioxidant coatings.

Acknowledgment

Authors are grateful to the Center for Scientific and Technical Research in Physico-Chemical Analysis Ouargla (C.R.A.P.C), Laboratory of Sahara Geology and Laboratory of Dynamics, Interaction and Reactivity of Systems Ouargla for their great contribution in the realization of this work.

Declarations

EthicalApproval:not applicable
Consent to Participate:not applicable
Consent to Publish:not applicable

Competing interests: The authors declare no competing interests.

Conflict of Interest: The authors declare that they have no conflict of interest.

Author contribution: Conceptualization, MB.G, FZ.A; methodology, MB.G, S.Z; investigation, MB.G, Z.M ; resources MB.G, Z.M; data curation; MB.G; writing—original draft preparation, MB.G, S.Z, Z.M —review and editing, MB.G, S.Z, Z.M ; supervision, FZ.A; project administration, MB.G; All authors have readand agreed to the published version of the manuscript.

Funding : This research received no specific grant from any funding agency in the public, commercial, or not-for-profit sectors

Availability of data and materials : not applicable

References

1 Ramsden, J., *Nanotechnology: an introduction*. 2016: William Andrew.

2 Nascimento, J., et al., *New advances of the nanotechnology in textile engineering: functional finishing with quantum dots and others nanoparticles*, in *Nanomaterials and Nanotechnology*. 2021, Springer. p. 239-281.

3. Singh, S., P. Rajesh, and Y. Ravindra, *Study And Evaluation Of The Microorganisms For The Formation Of Metal Nanoparticles And Their Application.* Journal of Positive School Psychology, 2022: p. 4425-4433.

4. Oves, M., et al., *Green synthesis of silver nanoparticles by Conocarpus Lancifolius plant extract and their antimicrobial and anticancer activities.* Saudi Journal of Biological Sciences, 2022. **29**(1): p. 460-471.

5. Salgado, P., et al., *Green synthesis of Ag/Ag2O nanoparticles on cellulose paper and cotton fabric using Eucalyptus globulus leaf extracts: toward the clarification of formation mechanism.* Surfaces and Interfaces, 2023: p. 102928.

6. Patil, D.M., et al., *Synthesis of Ag-Ag2O nanoparticles using Ageratum conyzoides leaf extract for the catalytic reduction of nitrobenzene and methylene blue and antibacterial applications.* Iranian Journal of Catalysis, 2023. **13**(1): p. 47-56.

7. Anandalakshmi, K., J. Venugobal, and V. Ramasamy, *Characterization of silver nanoparticles by green synthesis method using Pedalium murex leaf extract and their antibacterial activity.* Applied Nanoscience, 2016. **6**(3): p. 399-408.

8. Bouafia, A. and S.E. Laouini, *Green synthesis of iron oxide nanoparticles by aqueous leaves extract of Mentha Pulegium L.: Effect of ferric chloride concentration on the type of product.* Materials Letters, 2020. **265**: p. 127364.

9. Mighri, H., et al., *Antimicrobial and antioxidant activities of Artemisia herba-alba essential oil cultivated in Tunisian arid zone.* Comptes Rendus Chimie, 2010. **13**(3): p. 380-386.

10. Braca, A., et al., *Antioxidant activity of flavonoids from Licania licaniaeflora.* Journal of ethnopharmacology, 2002. **79**(3): p. 379-381.

11. Oyaizu, M., *Studies on products of browning reaction.* The Japanese journal of nutrition and dietetics, 1986. **44**(6): p. 307-315.

12. Piaru, S.P., et al., *Antioxidant and antiangiogenic activities of the essential oils of Myristica fragrans and Morinda citrifolia.* Asian Pac J Trop Med, 2012. **5**(4): p. 294-298.

13. Singh, R., M.A.M. Shushni, and A. Belkheir, *Antibacterial and antioxidant activities of Mentha piperita L.* Arabian Journal of Chemistry, 2011.

14. Prieto, P., M. Pineda, and M. Aguilar, *Spectrophotometric quantitation of antioxidant capacity through the formation of a phosphomolybdenum complex: specific application to the determination of vitamin E.* Analytical biochemistry, 1999. **269**(2): p. 337-341.

15. Uribe, E., et al., *Assessment of vacuum-dried peppermint (Mentha piperita L.) as a source of natural antioxidants.* Food chemistry, 2016. **190**: p. 559-565.

16. Masłowski, M., et al., *Potential application of peppermint (Mentha piperita L.), german chamomile (Matricaria chamomilla L.) and yarrow (Achillea millefolium L.) as active fillers in natural rubber biocomposites.* International Journal of Molecular Sciences, 2021. **22**(14): p. 7530.

17. Jurić, T., et al., *The evaluation of phenolic content, in vitro antioxidant and antibacterial activity of Mentha piperita extracts obtained by natural deep eutectic solvents.* Food Chemistry, 2021. **362**: p. 130226.

18. Hudz, N., et al., *Mentha piperita: Essential Oil and Extracts, Their Biological Activities, and Perspectives on the Development of New Medicinal and Cosmetic Products.* Molecules, 2023. **28**(21): p. 7444.

19. KS, S. and S. Shinde, *Phytochemical screening and evaluation of In-vitro antimicrobial properties of Mentha piperita L.* Int J Life Sci, 2019. **7**: p. 785-790.

20. Mainasara, M.M., et al., *Comparison of phytochemical, proximate and mineral composition of fresh and dried peppermint (Mentha piperita) leaves.* Journal of Science and Technology, 2018. **10**(2).

21. Gardia, D., et al., *Phytochemical analysis of Mentha piperita (Peppermint).* American Journal of Life Science Researches, 2023. **11**(1): p. 54-58.

22. Barhoum, A., et al., *Chapter 20 - Recent trends in nanostructured particles: synthesis, functionalization, and applications*, in *Fundamentals of Nanoparticles*, A. Barhoum and A.S. Hamdy Makhlouf, Editors. 2018, Elsevier. p. 605-639.

23. Zare, M., et al., *Novel Green Biomimetic Approach for Synthesis of ZnO-Ag Nanocomposite; Antimicrobial Activity against Food-borne Pathogen, Biocompatibility and Solar Photocatalysis.* Scientific Reports, 2019. **9**(1): p. 8303.

24. Naika, H.R., et al., *Green synthesis of CuO nanoparticles using Gloriosa superba L. extract and their antibacterial activity.* Journal of Taibah University for Science, 2015. **9**(1): p. 7-12.

25. Kumar, B., et al., *Andean Sacha Inchi (Plukenetia Volubilis L.) leaf-mediated synthesis of Cu2O nanoparticles: a low-cost approach.* Bioengineering, 2020. **7**(2): p. 54.

26. Mwakalesi, A.J., *Green synthesis of silver nanoparticles using aqueous extract of vachellia xanthophloea and their potential use for antibacterial and sensing of mercury ions.* Plasmonics, 2023: p. 1-14.

27. Strehlow, W. and E.L. Cook, *Compilation of energy band gaps in elemental and binary compound semiconductors and insulators.* Journal of Physical and Chemical Reference Data, 1973. **2**(1): p. 163-200.

28. Jayaprakash, P., M.P. Mohamed, and M.L. Caroline, *Growth, spectral and optical characterization of a novel nonlinear optical organic material: d-Alanine dl-Mandelic acid single crystal.* Journal of Molecular Structure, 2017. **1134**: p. 67-77.

29. Mallick, P. and B. Dash, *X-ray diffraction and UV-visible characterizations of α-Fe2O3 nanoparticles annealed at different temperature.* Nanosci. Nanotechnol, 2013. **3**(5): p. 130-134.

30. Yang, Y., et al., *Cu2O/CuO bilayered composite as a high-efficiency photocathode for photoelectrochemical hydrogen evolution reaction.* Scientific reports, 2016. **6**(1): p. 1-13.

31. Gaffar, M., A.A. El-Fadl, and S.B. Anooz, *Influence of strontium doping on the indirect band gap and optical constants of ammonium zinc chloride crystals.* Physica B: Condensed Matter, 2003. **327**(1): p. 43-54.

32. Liu, D., et al., *Indirect-to-direct band gap transition and optical properties of metal alloys of Cs 2 Te 1− x Ti x I 6: a theoretical study.* RSC advances, 2020. **10**(60): p. 36734-36740.

33. Shah, W.H., et al., *Tuning of the band gap and dielectric loss factor by Mn doping of Zn1-xMnxO nanoparticles.* Scientific Reports, 2023. **13**(1): p. 8646.

34. Martienssen, W., *Über die excitonenbanden der alkalihalogenidkristalle.* Journal of Physics and Chemistry of Solids, 1957. **2**(4): p. 257-267.

35. Masikini, M., *The use of cyclodextrin template-based metal oxide nanomaterials in the development of electrochemical sensors for phenolic endocrine disruptor compounds.* 2010, University of the Western Cape.

36. Pawar, O., et al., *Green synthesis of silver nanoparticles from purple acid phosphatase apoenzyme isolated from a new source Limonia acidissima.* Journal of Experimental Nanoscience, 2016. **11**(1): p. 28-37.

37. Yassin, M.T., et al., *Facile Green Synthesis of Silver Nanoparticles Using Aqueous Leaf Extract of Origanum majorana with Potential Bioactivity against Multidrug Resistant Bacterial Strains.* Crystals, 2022. **12**(5): p. 603.

38. Djamila, B., et al., *In vitro antioxidant activities of copper mixed oxide (CuO/Cu2O) nanoparticles produced from the leaves of Phoenix dactylifera L.* Biomass Conversion and Biorefinery, 2022: p. 1-14.

39. Abdullah, J.A.A., et al., *Green synthesis and characterization of iron oxide nanoparticles by pheonix dactylifera leaf extract and evaluation of their antioxidant activity.* Sustainable Chemistry and Pharmacy, 2020. **17**: p. 100280.

40. Bouafia, A., et al., *Green biosynthesis and physicochemical characterization of Fe3O4 nanoparticles using Punica granatum L. fruit peel extract for optoelectronic applications.* Textile Research Journal, 2022. **92**(15-16): p. 2685-2696.

41. Kohan Baghkheirati, E., et al., *Synthesis and antibacterial activity of stable bio-conjugated nanoparticles mediated by walnut (Juglans regia) green husk extract.* Journal of Experimental Nanoscience, 2016. **11**(7): p. 512-517.

42. Meng, Y., *A sustainable approach to fabricating Ag nanoparticles/PVA hybrid nanofiber and its catalytic activity.* Nanomaterials, 2015. **5**(2): p. 1124-1135.

43. Rajabi, A., et al., *Development and antibacterial application of nanocomposites: Effects of molar ratio on Ag2O–CuO nanocomposite synthesised via the microwave-assisted route.* Ceramics International, 2018. **44**(17): p. 21591-21598.

44. Klug, H.P. and L.E. Alexander, *X-ray diffraction procedures: for polycrystalline and amorphous materials*. 1974.

45. Moya, C., X. Batlle, and A. Labarta, *The effect of oleic acid on the synthesis of Fe 3− x O 4 nanoparticles over a wide size range.* Physical Chemistry Chemical Physics, 2015. **17**(41): p. 27373-27379.

46. Dehsari, H.S., et al., *Effect of precursor concentration on size evolution of iron oxide nanoparticles.* CrystEngComm, 2017. **19**(44): p. 6694-6702.

47. Laouini, S., A. Bouafia, and M. Tedjani, *Catalytic activity for dye degradation and characterization of silver/silver oxide nanoparticles green synthesized by aqueous leaves extract of Phoenix dactylifera L.* 2021.

48. Munteanu, I.G. and C. Apetrei, *Analytical methods used in determining antioxidant activity: A review.* International Journal of Molecular Sciences, 2021. **22**(7): p. 3380.

49. Marchi, R.C., et al., *Chemical implications and considerations on techniques used to assess the in vitro antioxidant activity of coordination compounds.* Coordination Chemistry Reviews, 2022. **451**: p. 214275.

50. Gulcin, İ. and S.H. Alwasel, *DPPH radical scavenging assay.* Processes, 2023. **11**(8): p. 2248.

51. Li, K., et al., *Recent advances in lignin antioxidant: Antioxidant mechanism, evaluation methods, influence factors and various applications.* International Journal of Biological Macromolecules, 2023: p. 125992.

52. Brand-Williams W, et al., *Use of a free radical method to evaluate antioxidant activity.* Lebensmittel- Wissenschaft und -Technologie., 1995. **28**: p. 25-30.

53. ABIDET, A., et al., *Assessment of total phenolics and flavonoids, and evaluation of scavenging activity of the aerial parts of Verbascum thapsus L. and Lactuca virosa L. grown in Algeria.* 2020.

54. Goudjil, M.B., et al., *Biological activities of essential oils extracted from Thymus capitatus (Lamiaceae).* South African Journal of Botany, 2020. **128**: p. 274-282.

55. Hamada Saoud, D., et al., *Phytochemical screening of aerial organs of wild fennel essential oils from southeast Algeria: identification of chemical composition, antioxidant, and antimicrobial activities.* Biomass Conversion and Biorefinery, 2023.

56. Polat Kose, L. and İ. Gulcin, *Evaluation of the antioxidant and antiradical properties of some phyto and mammalian lignans.* Molecules, 2021. **26**(23): p. 7099.

57. Saroyo, H. and I.A.N. Arifah, *Antioxidant activity using DPPH & FRAP method and their correlation with the levels of phenolic and flavonoid compounds from nemba plants (Azadirachta Indica A. Juss).* Journal of Nutraceuticals and Herbal Medicine, 2021. **3**(2): p. 10-20.

58. Oracz, J., et al., *Bioactive Compounds, Antioxidant Activity and Sensory Properties of Northern Red Oak (Quercus rubra L., syn. Q. borealis F. Michx) Seeds Affected by Roasting Conditions.* Molecules, 2023. **28**(5): p. 2299.

59. Cherrat, L., et al., *Chemical composition and antioxidant properties of Laurus nobilis L. and Myrtus communis L. essential oils from Morocco and evaluation of their antimicrobial activity acting alone or in combined processes for food preservation.* Journal of the science of food and agriculture, 2014. **94**(6): p. 1197-1204.

60. Balasundram, N., et al., *Antioxidant properties of palm fruit extracts.* Asia Pacific journal of clinical nutrition, 2005. **14**(4): p. 319.

61. Yi, Z., et al., *In vitro antioxidant and antimicrobial activities of the extract of Pericarpium Citri Reticulatae of a new Citrus cultivar and its main flavonoids.* LWT-Food Science and technology, 2008. **41**(4): p. 597-603.

62. Mahlangeni, N.T., et al., *Biogenic synthesis, antioxidant and antimicrobial activity of silver and manganese dioxide nanoparticles using Cussonia zuluensis Strey.* Chemical Papers, 2020. **74**(12): p. 4253-4265.

63. Mohd Yusof, H., et al., *Microbial Mediated Synthesis of Silver Nanoparticles by Lactobacillus Plantarum TA4 and its Antibacterial and Antioxidant Activity.* Applied Sciences, 2020. **10**(19): p. 6973.

64. Dridi, R., et al., *Biosynthesized silver nanoparticles using Anagallis monelli: Evaluation of antioxidant activity, antibacterial and antifungal effects.* Journal of Molecular Structure, 2022. **1251**: p. 132076.